International Journal of Forest Engineering

ISSN: 1494-2119 (Print) 1913-2220 (Online) Journal homepage: www.tandfonline.com/journals/tife20

Integrating soil, weather, and lightweight deflectometer data for dynamic bearing-capacity estimates on forest roads

Joel Kostensalo, Perttu Anttila, Alwin Hardenbol & Kari Väätäinen

To cite this article: Joel Kostensalo, Perttu Anttila, Alwin Hardenbol & Kari Väätäinen (08 Jul 2026): Integrating soil, weather, and lightweight deflectometer data for dynamic bearing-capacity estimates on forest roads, International Journal of Forest Engineering, DOI: 10.1080/14942119.2026.2698172

To link to this article: https://doi.org/10.1080/14942119.2026.2698172

INTERNATIONAL JOURNAL OF FOREST ENGINEERING
https://doi.org/10.1080/14942119.2026.2698172

Integrating soil, weather, and lightweight deflectometer data for dynamic bearing-capacity estimates on forest roads

Joel Kostensalo[a], Perttu Anttila[b], Alwin Hardenbol[a], and Kari Väätäinen[b]

[a]Department of Natural Resources, Natural Resources Institute Finland, Joensuu, Finland; [b]Production Systems, Natural Resources Institute Finland, Helsinki, Finland

ABSTRACT

Trafficable forest roads are vital for providing timber for the forest industry. Dynamic trafficability models for forest roads are needed, because many forest roads are trafficable for only some part of the year. We studied 10 road segments in eastern Finland during non-frozen periods, collecting E-modulus measurements using a lightweight deflectometer from 2023 to 2025. Approximately 15.1% of variation in bearing capacity was between road segments, 8.4% within road segments, and 76.5% was dynamic, indicating that the theoretical maximal performance of static models would be limited to explaining 23.5% of the variation. Prediction models were built utilizing weather station data and openly available soil type information on subsoils. We found that moving averages of ambient temperature and rainfall can capture dynamic variation in bearing capacity. Re-graveling and surface freezing increase the bearing capacity precipitously. Systematic differences between road segments can be captured by calibrating the models. We found robust evidence that two calibration measurements carried out at separate times significantly improve predictions, while additional measurements provide little to no value.

ARTICLE HISTORY
Received 14 April 2026
Accepted 29 June 2026

KEYWORDS
Gravel road; trafficability; E-modulus; dynamic modeling

Introduction

Trafficable forest roads and private gravel roads are vital for sustainable, cost-effective, and year-round delivery of timber for the forest industry. These roads are also used, e.g. for defense and emergency services. Roads must have sufficient bearing capacity to support the weight of vehicles and withstand traffic without undue damage to the road. This is a significant concern especially in Finland where the total length of private roads is approximately 350,000 km, of which 157,000 km are forest roads (Greis et al. 2019). Furthermore, the allowable gross vehicle mass of 76 metric tons is high by international standards (Kärhä et al. 2024). Yet most of the forest road network was built in the period 1960–1990 for lighter trucks, and the roads are deteriorating partly due to the relatively high renovation and maintenance costs and a shortage of public funding for this work (Kaakkurivaara 2018). Driving on roads with a low bearing capacity can result in significant rutting, or even damage to the structure of the road, which can necessitate costly renovations. Accurate, real-time information on road trafficability is needed by logistics planners and truck drivers to mitigate these issues without undue halting of traffic for extended periods of time.

Currently, drivers and planners rely on local knowledge and static estimates (e.g. papiNet 2025) when evaluating the trafficability of a given forest road. Recently, static condition and bearing capacity models have been developed for private gravel road segments. Bergqvist et al. (2024) developed bearing capacity prediction models based on soil type and a soil moisture index. Light Detection and Ranging (LiDAR) data have been used to estimate vegetation cover along road segments (Waga et al. 2020), as well as the structural condition, surface wearing, and flatness (Waga et al. 2021). Karjalainen et al. (2025) used field-measured road width, ditch depth, depth-to-water index, soil type, and variables based on gamma-ray spectrometry to predict bearing capacities. Even an operational classification of road condition based on LiDAR data has been published by the Finnish Forest Center (Yksityisteiden karttapalvelut, 2026). However, the fundamental limitation of static prediction models is that the trafficability of forest roads is highly weather dependent. Roads which are generally in poor condition may be trafficable only in dry summer conditions or when the road is frozen, and even roads in good condition may become untrafficable for some part of the year.

The effect of weather on the bearing capacity of gravel roads is well understood at a general level. Water in road structures softens them and increases the accumulation of permanent deformation (Saevarsdottir and Erlingsson 2013). Thus, the spring thaw period, periods of heavy rainfall (Grajewski 2016), and wet roads in late autumn have been identified as particularly risky conditions. Moreover, the material composition of the road structure, the thickness of its constituent layers (O'Mahony et al. 2000), and the sub-soil type, besides influencing the bearing capacity directly, also affect weather sensitivity of the road. To address this issue, there is an ongoing shift from static prediction to dynamic, i.e., (near) real-time models based on weather data. Kestler et al. (2007, 2011) compared the identification of spring thaw periods using lightweight

CONTACT Joel Kostensalo joel.kostensalo@luke.fi Department of Natural Resources, Natural Resources Institute Finland, Yliopistokatu 6B, Joensuu FI-80100, Finland

Supplemental data for this article can be accessed online at https://doi.org/10.1080/14942119.2026.2698172

deflectometers and thaw-prediction models among other models to optimize load restrictions. Fjeld et al. (2024) found that bearing-capacity estimation can be improved with radar-satellite data which captures information of (past) soil-moisture condition. However, we did not find any published studies where weather variables have been used to explain bearing capacity. Whereas satellite-based information reflects past road conditions, future conditions could be predicted with the aid of weather forecasts. Väätäinen et al. (2025) sought to establish a basis for investigating the relationship between weather conditions, road type, road characteristics, and bearing capacity by establishing a longitudinal research design consisting of several test segments with weather stations and frequent bearing-capacity measurements with light falling weight deflectometers (LWDs), which are highly mobile and affordable. While the impact of an LWD on the ground is significantly smaller than that of a traditional falling weight deflectometer, which is generally commensurate with the mass effect of a single axle of a loaded timber truck, the measurements tend to be highly correlated (Kaakkurivaara et al. 2015). This experimental setup is the basis of this work.

The aim of this study was to develop the first ever dynamic bearing capacity model for gravel roads using eastern Finland as a pilot case. Both dynamic (weather data) and static (soil type) explanatory variables were utilized. A further aim was to test if "calibration" (i.e. adjusting predictions based on a few LWD measurements) could significantly improve bearing capacity estimates. If accurate enough, this study would demonstrate that it is possible to build dynamic bearing-capacity models which could be used for optimizing traffic, maintenance, and renovation of forest roads.

Materials and methods

Road data

The road data were measured from 10 approximately 100-m-long gravel road segments (80 to 120 m) forming four distinct clusters (A–D) in eastern Finland (approx. 62.67° N 29.08° E) between 2023 and 2025. The locations of the segments are presented in Figure 1 (see also Väätäinen et al. 2025). The

Figure 1. Locations of the 10 road segments and four clusters in the study.

Table 1. Road segments, clusters with the same weather station, and subsoil types present in the segment.

Road segment	Cluster	Soil type
1	A	Carex peat / sand
2	A	Carex peat
3	B	Sandy moraine
4	B	Clay
5	C	Sandy moraine
6	C	Carex peat / sandy moraine
7	D	Sand
8	D	Fine sand
9	D	Gravel
10	A	Sandy moraine

subsoils and road conditions of the road segments were representative of typical forest road conditions in eastern Finland. For each segment, subsoil type was determined based on open-source data on superficial deposits in Finland provided by the Geological Survey of Finland (GTK 2018) (see Table 1). A detailed soil analysis for each road segment can be found in Väätäinen et al. (2025). However, as such precise data would not be available in large-scale application, using these measurements in evaluating the models would result in an overly optimistic picture about how well the models work. The segments were geographically clustered, and each cluster consisted of two or three segments less than 1 kilometer apart. Each cluster had a weather station (Vaisala WXT530) which recorded air temperature and rainfall on an hourly basis, and the information was sent and stored to a server. Bearing capacity of the road segments was measured using a Light Falling Weight Deflectometer (LWD) Zorn ZFG 3.1. With the LWD, the bearing capacity in megapascals was recorded at 10–20 m intervals. At every interval, a measurement point was located on both wheel paths. A more detailed description of the road measurements can be found in Väätäinen et al. (2025). Approximately 3400 observations from 10 different road segments on 39 separate days were collected (12 to 14 locations at a time per segment, left and right side of the road, typically 0, 20, 40, 60, 80, and 100 m from the starting point). Due to logistical limitations, all road segments could not be measured on the same day. On 17 occasions, all road segments were measured during the same day, 5 times one segment was missed, 5 times two clusters were measured,13 times two clusters were measured, 3 times one cluster was measured. However, the exact time of measurement was always recorded, so that the precise weather conditions could be determined accurately. The median time difference between measurements for a given segment was 9 days (range 1–314 days, mean 28 days).

Statistical analysis

First, we examined how much of the variation in bearing capacity is due to variation between road segments, how much between specific locations within road segments, and how much of it is residual variation (i.e. dynamic + small measurement error). This was done using two-way nested analysis of variance (ANOVA).

The roles of temperature, rainfall, soil type, and their interactions were investigated using linear mixed-effects models. For temperature, we used a moving average of the last

72 hours measured in centigrade without allowing it to fall below zero. For rainfall, we used a 48-hour moving average in mm. For a justification of the moving window sizes see Väätäinen et al. (2025). There were a handful (<0.01%) of rainfall observations with extreme values, exceeding 1000 mm/h as well as some negative values. To mitigate the effect of these erroneous values, all negative values were set to zero and any rainfall value exceeding 20 mm/h was set to exactly 20 mm/h (heavy rainfall caused some coarse errors where the device could report hourly rainfall up to 1000 mm/h). The rainfall detector for Cluster A was known to be faulty, giving systematically too high values (see Väätäinen et al. 2025), approximately four times higher than the other devices despite being geographically close. Thus, the readings from this device were rescaled so that the mean corresponded to the mean of the other devices. As a sensitivity analysis, we also ran the results without these corrections, and interestingly the results were almost identical, changing only modestly, while the conclusions were unaffected. We tested five different model variations starting with a simple model without interactions and then adding either one, two, or three interactions with soil type. The models can be formally written as Equations 1–5:

$$E_{i,j} = \Sigma\beta_S S_{i,j} + \beta_r \mathrm{R}_i + \beta_T \mathrm{T}_i + \beta_F F_i + \beta_{RG} RG_i + \eta_i + \theta_{i,j} + \epsilon_{i,j} = \text{base model} \tag{1}$$

$$E_{i,j} = \text{base model} + \Sigma\beta_{ST} S_{i,j} \mathrm{T}_i \tag{2}$$

$$E_{i,j} = \text{base model} + \Sigma\beta_{SR} S_{i,j} \mathrm{R}_i + \Sigma\beta_{ST} S_{i,j} \mathrm{T}_i + \Sigma\beta_{SRT} S_{i,j} \mathrm{T}_i \mathrm{R}_i \tag{3}$$

$$E_{i,j} = \text{base model} + \Sigma\beta_{SR} S_{i,j} \mathrm{R}_i \tag{4}$$

$$E_{i,j} = \text{base model} + \Sigma\beta_{ST} S_{i,j} \mathrm{T}_i, \tag{5}$$

where $E_{i,j}$ is the E-modulus of road segment i at location j, $S_{i,j}$ is the soil type with summation Σ happening over all possible soil types, R_i the 48-hour smoothed rainfall, T_i the 72-hour smoothed temperature, F_i is a freezing indicator which is one if the average temperature is negative for the past 8 hours and zero otherwise, RG_i is a dummy variable accounting for re-gravelling (segments 3 and 4 in June 2024), β' s are the regression coefficients for the fixed effects, η_i is a random effect for the road segment i, $\theta_{i,j}$ is a random effect for the location j on the road segment i, and $_{i,j}$ is an error term. The random effects and error terms are assumed to be independent and normally distributed. All models were fitted using residual maximum likelihood. The re-gravelling event was visually noticed by the measurement crew and was noted to consist of adding an approximately 5 cm layer of 0–16 or 0–32 mm gravel, which is a typical maintenance method in Finland. Further details are unknown to the authors.

The optimal number of calibration visits (i.e. on-location measurement events) and the best model were estimated using a cross-validation approach, where the model was trained on nine of the road segments and tested on the one remaining segment. As there were exactly 10 segments, the cross-validation is simultaneously both leave-one-out and a 10-fold cross-validation. For a discussion on cross-validation see, e.g, Stone (1974). As road segments 4, 8, and 9 had soil types which were not present in other segments, we assumed that the soil type was "sand soil" for the model fit, which was the reference level of the model. The calibration was based on the first measurements of the road segment by subtracting the average prediction error of the model for the specific segment. We tested calibration based on 1, 2, 3, 4, or 5 visits. The optimal number of calibration visits was chosen based on the root-mean squared error of the predictions with predictions made at the level of a specific location on the segment. The predictive power of the model was then tested at the road-segment level using the same cross-validation approach with 1) no calibration and 2) the chosen "optimal" number of calibration visits. The quality was assessed by graphically investigating how well the trends are qualitatively reproduced and quantitively using root mean squared error (RMSE) of predicted bearing capacity. As some of the measurements were close together in time (about 25% of the measurements were done within 1 week of the previous one) there may be autocorrelation between the measurements, which should be accounted for. Thus, we tried introducing autocorrelation into the model in two forms: with a first-order autoregressive structure (AR(1)) and with a linear-in-time autocorrelation structure. However, these models lead to slightly higher RMSE values and were thus not used in the final model.

To test how well low bearing capacity could be predicted, we classified the predictions into above or below a certain limit value. The limit value was varied between 1 and 100 MPa. We used the traditional classification metrics "precision" (true positive/(true positive + false positive)) and "recall" (true positive/(true positive + false negative)), where a "true positive" means that the model predicts an E-modulus below the limit value and the field measurements are in agreement, "false negative" means that the bearing capacity is below the limit value but the model predicts a value over the limit, and a "false positive" means that the model predicts that the bearing capacity is below the limit value but according to field measurements the bearing capacity is above the limit.

All results were evaluated at the road-segment level, i.e. looking at the values averaged over all 12 measurement locations. This is because rainfall and temperature values are the same, not only for a road segment, but for each road segment cluster. Furthermore, for eight of the road segments there is only one soil type present and for the other two segments there are two soil types. Thus, there are no variables which could even theoretically capture variation within a given road segment. Model fitting and relevant inferences were carried out using the R-package nlme (Pinheiro and Bates 2024). All statistical analyses were carried out using the statistical software R (R Core Team 2024).

Results

The average bearing capacity of a road segment measurement was 38.0 MPa with a standard deviation of 20.3 and a range of 2.8–258.6. When averaged at the road-segment level, the average was 38.2 with a standard deviation of 16.5 and a range of

5.7–113.1. There is thus more dynamic variation within a road segment than between road segments. Based on ANOVA, 15.1% of the variation in the data was between road segments and 8.4% between specific locations on the road segments, which leaves 76.5% for dynamic variation driven by weather conditions including a small measurement error component. Over the 3 years, the average air temperature was +3.3°C (SD 11°C, ranging from −39°C to +32°C) and the hourly rainfall on average 0.052 mm (SD 0.39 mm, ranging from 0 mm to 20 mm). At the LWD measurement times, the 72-h smoothed non-negative temperature was on average 9.7°C (SD 6.1°C, range 0–23.2°C) and the 48-h smoothed rainfall was on average 0.10 mm (SD 0.16 mm, range 0–0.75 mm). The distribution of bearing capacities, and the original time series of temperature and rainfall are presented graphically in the Supplementary material (see Figure S1–S5).

The results regarding the number of calibration visits are presented in Figure 2. All five models behave in a very similar way with respect to the number of calibration visits: The first visit improves the predictions a little bit, then there is a huge jump in performance following the second calibration visit, after which the value of an additional calibration measurement diminishes significantly and the fourth and fifth visit do not provide any additional value. The model defined by Eq. (2) (interaction with soil and temperature) performed the best in the cross validation.

The fixed effects alone can explain 30% of the total variance based on the linear mixed-effects model. When road segment and specific location are also included, the full model can

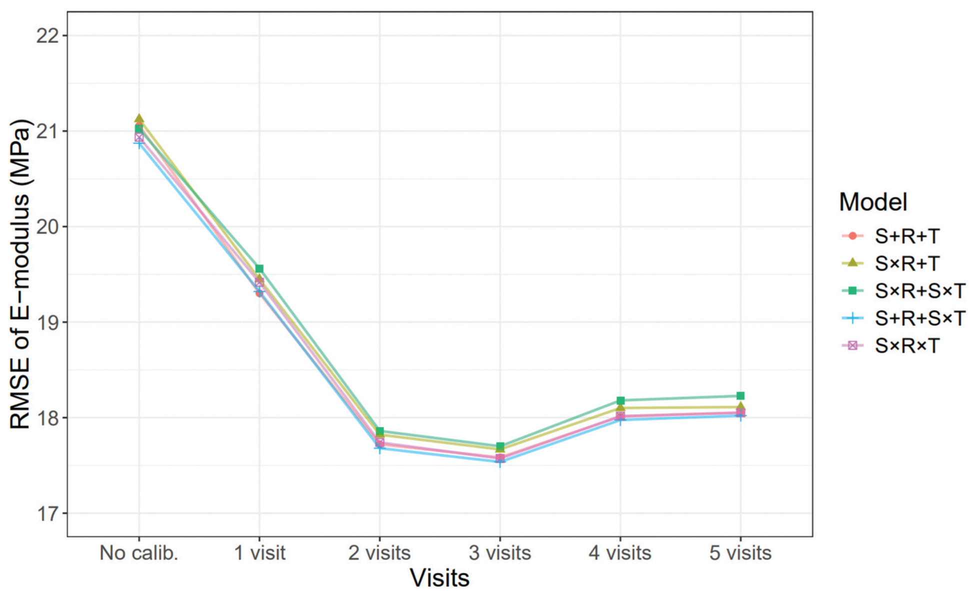

Figure 2. Number of calibration visits and the root mean squared error (RMSE) of bearing capacity (E-modulus) for different variations of a linear mixed-effects model.

Table 2. Fixed and random effects for the best model (linear model with no interactions S+R+T) fitted to the full data.

Model component	Variable	Estimate	SE	*p*-value
Fixed effects	Intercept term	15.68	5.38	0.004
	Temperature (72 h)	1.25	0.11	<0.0001
	Rainfall (48 h)	−0.35	1.32	0.79
	Soil type			
	Sandy soil (reference)			
	Sandy moraine	12.92	5.91	0.03
	Fine sand	9.48	12.03	0.46
	Carex peat	5.18	3.69	0.16
	Clay	−10.57	12.06	0.41
	Gravel	19.16	12.04	0.16
	Soil type × Temperature (72 h)			
	Sandy soil (reference)			
	Sandy moraine	0.13	0.13	0.32
	Fine sand	0.41	0.16	0.01
	Carex peat	−0.29	0.14	0.04
	Clay	0.31	0.16	0.06
	Gravel	0.17	0.17	0.32
	Freezing (8 h)	37.84	1.28	<0.0001
	Re-graveling	8.86	0.95	<0.0001
Random effects	Road segment	σ = 10.59		
	Specific location (side, distance)	σ = 5.18		
	Residual	σ = 15.33		
Fit quality	$R^2_{mar}/R^2_{con} = 0.30/0.56$			

explain 56% of the variance in bearing capacity. The 26% captured by the random effects is consistent with the ANOVA results showing that 23.5% of the variation is between road segments and specific locations, and that the variation between road segments (σ = 10.59) is about twice as large as within-segment variation (σ = 5.18). In the model, a one degree increase in temperature corresponds to a 1.25 MPa increase in bearing capacity (Table 2). One millimeter of additional rainfall in a 48-hour period is associated with a 0.35 MPa reduction in bearing capacity, while re-graveling and the road surface freezing significantly increase the bearing capacity. Sandy moraine provides on average 12.92 MPa more bearing capacity compared to sandy soil. Furthermore, fine sand ($p = 0.04$) and potentially clay ($p = 0.06$) harden and provide higher bearing capacities at higher temperatures, whereas the bearing capacity of carex peat does not improve as much as that of sandy soil at higher temperatures.

The cross-validation results for the road segments are presented in Figures 3 and 4. In general, the predicted dynamical behavior follows the trend of the E-modulus-measurements for all road segments. The uncalibrated results correlate weakly with the field measurements ($r = 0.34$), while the correlation between field measurements and calibrated results is moderate ($r = 0.68$). However, the predictions tend to have slightly less variation than the ground measurements, where especially the minima and maxima tend to be over- and underpredicted, respectively. The calibration (based on the first two visits) appears to improve the results significantly for segments 2, 7, 8, and 9, and moderately for segments 1, 4, and 10, while having little effect on segments 3, 5, and 6. It should be noted that for segments 4, 8, and 9 the soil type was unique and not available in the training data. Thus, the default prediction using the reference level "Sandy soil" may explain some of the advantage of a calibration measurement for these three segments. The first two measurements of road segment 10 were during the summer. The predictions seem to work well during this season, but there is significant underestimation in April. The re-graveling of segments 3 and 4 (location B) in June 2024 is reasonably well captured. This change is captured by the LWD. In locations B and D there is a sharp jump in April 2024, which corresponds to the road

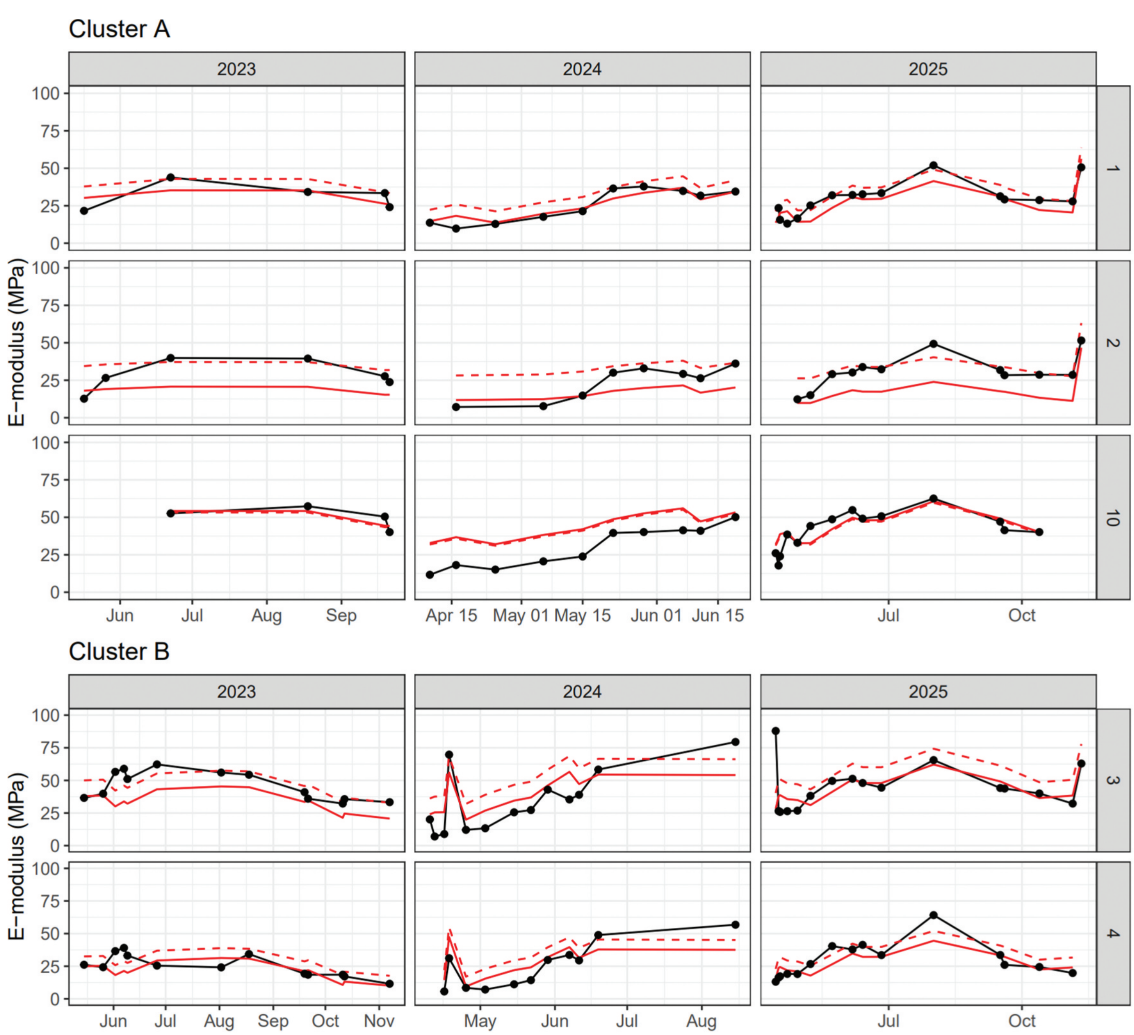

Figure 3. The average E-modulus of the road segments 1–4 and 10 (segment number on the right-hand side), and predictions without calibration and with calibration based on the first two visits. Cluster A is formed by segments 1, 2, and 10 and Cluster B by segments 3 and 4 (see Figure 1 for a map). The black dots represent LWD measurements, the dashed red line represents the uncalibrated predictions, and the solid red line represents predictions calibrated results.

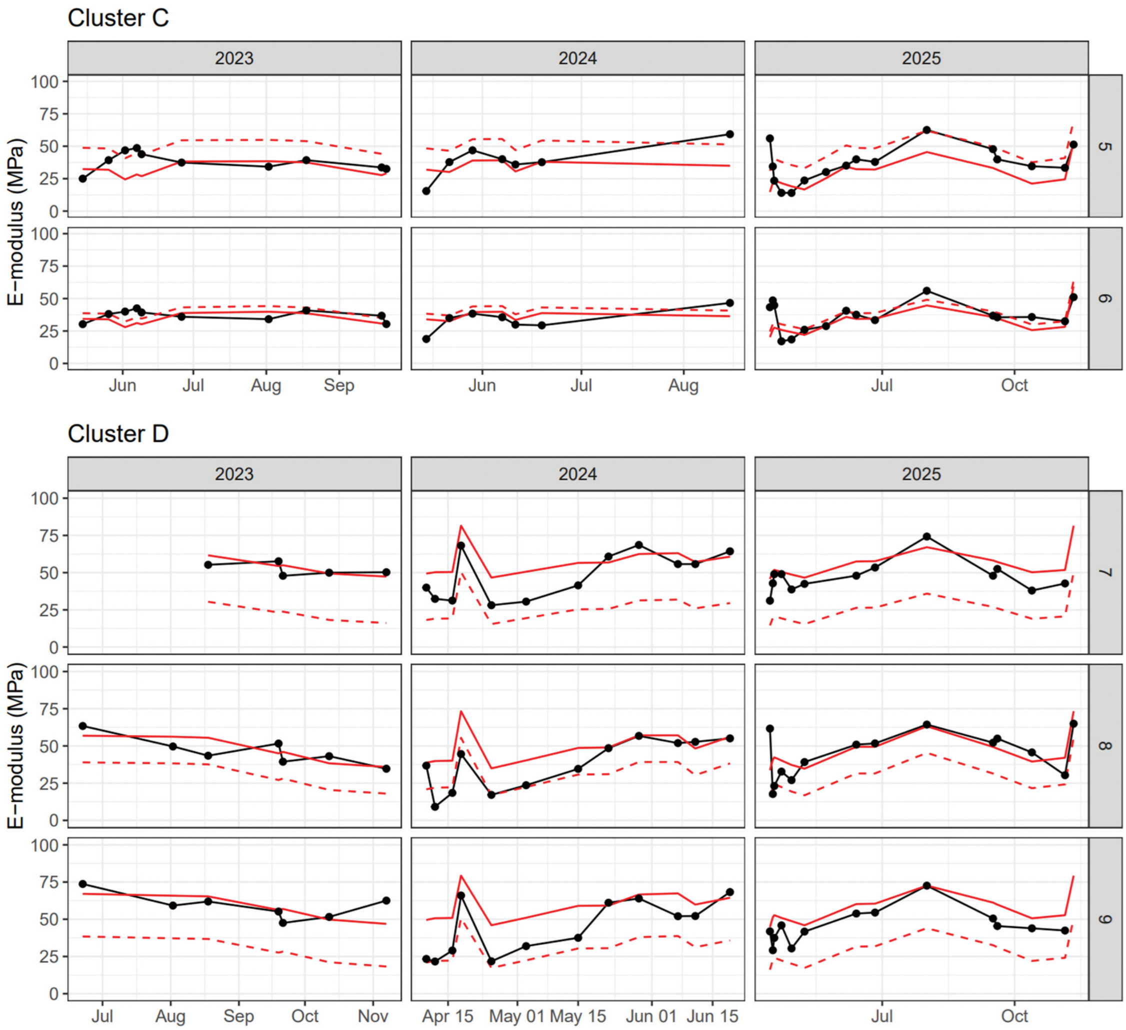

Figure 4. The average E-modulus of the road segments 5–9 (segment number on the right-hand side) and predictions without calibration and with calibration based on the first two visits. Cluster C is formed by segments 5 and 6 and Cluster D by segments 7, 8, and 9 (see Figure 1 for a map). The black dots represent LWD measurements, the dashed red line represents the uncalibrated predictions, and the solid red line represents predictions calibrated results.

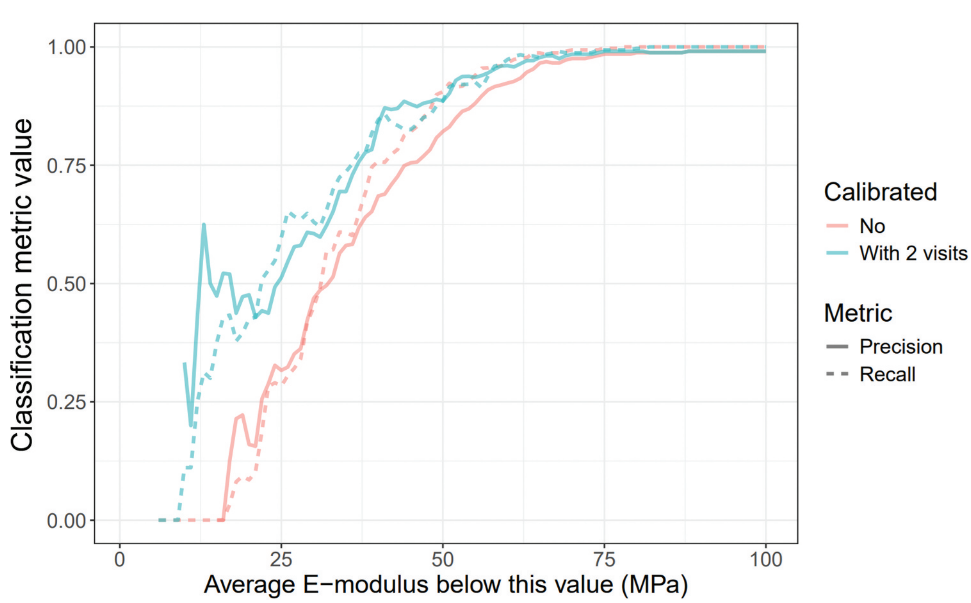

Figure 5. Precision and recall for classifying bearing capacity into low bearing capacity (average E-modulus below given limit value) and high bearing capacity (average E-modulus above the limit).

freezing, and is captured well by the model. In general, the prediction errors show some but not severe autocorrelation (see Supplementary material Figure S6).

Results for classifying road segments at a given time into low bearing capacity and high bearing capacity are presented in Figure 5. When the model is not calibrated, precision and recall exceed 0.50 at 33 MPa, while with a calibrated model 0.50 can be achieved for 20 MPa. Without calibration, precision is systematically lower than with calibration regardless of the chosen limit.

Discussion

This study has shown the feasibility of dynamically modeling the trafficability of forest roads. We found that 15.1% of the variation in bearing capacity was between road segments, 8.4% within road segments, while 76.5% was dynamicl. This indicates that a static model could only capture about 23.5% of the variation. Ambient temperature and rainfall were successfully incorporated in a prediction model of E-modulus. The coefficients of the model are in line with the phenology of gravel roads: rainfall lowers bearing capacity, while high temperatures, re-graveling, and freezing increase it. Grajewski (2016) showed in an experimental setting that heavy rainfall could lower the E-modulus by 16–25%, which is more than the regression coefficients of our models might on a first glance suggest. However, rainfall was associated with lower temperatures, and thus the effect is captured in the model mostly indirectly, mediated by temperature. According to Lehtonen et al. (2019) the time when forest roads are frozen on winter is projected to shorten by 1 month by 2050 in Finland. Likewise, Daniel et al. (2018) showed that the frozen period has shortened in the North-Eastern United States since the 1970s, and that climate modeling suggests that there will occasionally be winters without freezing in the latter half of the 21st century. Shifts and annual variation in the spring thaw and freezing periods necessitate the use of dynamic prediction models, as one can no longer rely on the road being frozen during the winter months.

Our sample included roads from a limited number of soil types. While these soil types cover a large part of the country, observations from other soil types are needed before the results can be generalized to the country level. The simple soil-type variable used in our models has the advantage that it can be determined based on an openly available map, but it should be kept in mind that, e.g. not all peat soils have the same bearing capacity. O'Mahony et al. (2000) showed using Irish data that the thickness of the peat layer is connected to the bearing capacity. By consequence, a 50 m resolution map of peat thickness covering the whole of Finland was recently published by Pohjankukka et al. (2025), which could be used as an additional input variable.

Calibration with two visits significantly improves the results regardless of the complexity of the model. A third visit may add a little extra information, but additional visits do not. The calibration should preferably be timed for spring or fall when the bearing capacity is low, as systematic errors for seasons with higher bearing capacity are not nearly as consequential as those during poor conditions. Calibration may need to be redone following any consequential changes, such as re-graveling or a major damage event. While the model includes re-graveling, it should be stressed that this was based on a single re-graveling event on two road segments which were located near each other. In cases where the road needs to be reconstructed, reconstruction should consider the fact that these are low-volume roads, but that the occasional traffic is mostly done with very heavy vehicles. For example, Miller et al. (2011) showed that in highway conditions full-depth reclamation may be an economical alternative for low-volume roads leading to similar bearing capacities as measured by a falling weight deflectometer.

As this study showed, during the low-bearing seasons in early spring or late autumn, the road may freeze slightly below the surface after a few days of freezing temperatures. This results in a rapid improvement in the road's bearing capacity. Our results indicate that a recently frozen road has on average 38 MPa higher bearing capacity than the same road prior to freezing. In our analysis, it seems that negative average temperature over the past 8 hours is sufficient for this effect. Further experiments need to be conducted to confirm this, but more accurate knowledge about sufficient freezing would facilitate better scheduling of heavy transport on forest roads.

In this study, we predicted bearing capacity at segment level. It is worth noticing that at location level the error is higher. This means that it is more difficult to predict individual weak locations on a road (which may stop traffic) than the average bearing capacity of a segment. However, we did find that very little of the average bearing capacity variation (8.4%) was within road segments. The modeling was based on measurements from road stations. In practical applications, however, the weather variables should be obtained from an open, wall-to-wall source (Open data, 2026). The reliability of predictions based on these data which have coarser spatial and temporal resolution should be tested. However, professional meteorological data is unlikely to suffer from the problems observed in our study, where the weather station reported unrealistic peaks in rainfall.

In practice, road bearing capacity is determined by a number of static and dynamic factors. The static factors include longitudinal road profile, thickness and material of the base course, and the soil type of subgrade. Transverse road profile, the depth and slope of ditches, verge formation, and vegetation shadow can be considered semi-dynamic as they may change over time, but not very often or rapidly. In addition to temperature and rainfall considered in this study, the dynamic factors include the frost line penetration depth and snow plowing. A potential data source for estimating additional static variables is the airborne laser scanning data by the National Land Survey of Finland (Laser scanning data 5 p, (2026). The inclusion of these variables would necessitate LWD measurements from many more road segments. On the other hand, caution needs to be exercised when increasing model complexity. It should also be noted that each road segment is unique, and the steepness and curvature vary. Further work utilizing laser scanning is needed to determine if such details could feasibly be included in an operational model.

Apart from dynamic modeling of the elastic modulus, further research is needed on the relationship between the elastic modulus and trafficability. According to the Finnish forest road instructions, the indicative bearing capacity for peat as a subgrade is 5 MPa (Metsäteho 2017). In such cases –

where roads are constructed over very low-supporting subgrades – special attention is required to ensure that the road structure meets the demands of heavy vehicle traffic (Munro 2004). Moreover, Kaakkurivaara (2018) reported a high risk of rutting when heavy vehicles traverse road segments with an E-modulus below 35 MPa, as measured by a lightweight deflectometer (LWD). However, a stress test with a laden timber truck on road segment 2 revealed no significant rutting even though the subgrade soil type was peat and the measured E-modulus was 25 MPa (Väätäinen et al. 2025). Comparison of these results cannot be made directly due to different types of LWDs in use. In addition, the road has been built following standards for road construction over peatland. In fact, a separate wooden mattress was settled in between peat and the road structure (Väätäinen et al. 2025).

Conclusions

Dynamic trafficability models for forest roads are needed, because many of them are trafficable for only some part of the year. Accurate, real-time information is needed to protect vulnerable road segments when bearing capacity is low, while not posing unnecessary and costly limitations to timber traffic by shutting down roads with sufficient bearing capacity. In addition to significant inter-annual variation, warming climate will gradually shift the length of the frozen period and timing of spring thaw, and thus planning based on past experience will become increasingly suboptimal. We have shown that rainfall, temperature (incl. freezing events), re-graveling, and soil type can be useful predictors for bearing capacity, but predictive power can be significantly improved with just two calibration measurements. LWDs are relatively low-cost and highly mobile, and could thus be easily used by ground crews in low-bearing capacity conditions to gather valuable data.

Further work is needed regarding real-world implementation and to generalize the model for a larger geographic area. Specifically, measurements from roads constructed on different soil types, and with varying thickness of layers (e.g. peat) are needed for a more granular prediction model.

Disclosure statement

No potential conflict of interest was reported by the author(s).

Funding

This study was part of the SecureLog project funded by Natural Resources Institute Finland (Luke) and the regionally funded project "Take Me Home Country Road," supported by European Union's regional and structural funds. These projects laid the foundation for automated online monitoring of road weather data and the establishment of road stations. PA and KV were supported by Northern Traffic Lights project funded by EU's Interreg Aurora programme in cooperation with Länsstyrelsen and Lapin Liitto [20370373]. JK and AH were supported by the Research Council of Finland [Grant No: 361209].

ORCID

Joel Kostensalo http://orcid.org/0000-0001-9883-1256

References

Bergqvist M, Davidsson A, Eliasson L. 2024. [A method for the interpretation of road accessibility class] En metod för förtolkning av vägens tillgänglighetsklass. Skogforsk Arbetsrapport. (1219–2024):22.

Daniel JS et al. 2018. Climate change: potential impacts on frost-thaw conditions and seasonal load restriction timing for low-volume roadways. Road Mater Pavement Des. 19(5):1126–1146. https://doi.org/10.1080/14680629.2017.1302355

Fjeld D, Persson M, Fransson JES, Bjerketvedt J, Bråthen M. 2024. Modelling forest road trafficability with satellite-based soil moisture variables. Int J Eng. 35(1):93–104. https://doi.org/10.1080/14942119.2023.2276628

Grajewski S. 2016. Influence of pavement moisture content on the load-bearing capacity of forest road. Infrastruct Ecol Rural Areas. IV:1451–1462.

Greis I., Perälä M., Perälä T. & Teppo M. editors. 2019. [Forest management recommendations for the upkeep of forest roads, a manual] Metsänhoidon suositukset metsäteiden kunnossapitoon, työopas. Tapion julkaisuja. 978-952-5632-78-1.

GTK. 2018. Superficial deposits 1: 20 000/1: 50 000; [accessed 2021 Nov 5]. https://tupa.gtk.fi/paikkatieto/meta/maapera_20_50k.html

Kaakkurivaara T. 2018. Innovative methods for measuring and improving the bearing capacity of forest roads. Diss For. 2018(251). https://doi.org/10.14214/df.251

Kaakkurivaara T, Vuorimies N, Kolisoja P, Uusitalo J. 2015. Applicability of portable tools in assessing the bearing capacity of forest roads. Silva Fenn. 49 (2) article id 1239.2). https://doi.org/10.14214/sf.1239

Kestler MA et al. 2007. Determining when to place and remove spring load restrictions on low-volume roads: three low-cost techniques. Transp Res Rec. 1989-2(1):219–229. https://doi.org/10.3141/1989-67

Kestler MA et al. 2011. Keeping springtime low-volume road damage to a minimum: toolkit of practical low-cost methods for road managers. Transp Res Rec. 2205(1):155–164. https://doi.org/10.3141/2205-20

Kärhä K et al. 2024. Overview of global long-distance road transportation of industrial roundwood. Croat J For Eng (Online). 45(1):217–236. https://crojfe.com/archive/upcoming-issue/overview-of-global-long-distance-road-transportation-of-industrial-roundwood/

Karjalainen V, Malinen J, Tokola T. 2025. Predicting bearing capacity and trafficability classes of forest roads using road properties and surrounding terrain information. Road Mater Pavement Des. 26(8):2037–2054. https://doi.org/10.1080/14680629.2024.2434945

Laser scanning data 5p. 2026. National Land Survey of Finland; [accessed 2026 Jun 22]. https://www.maanmittauslaitos.fi/en/maps-and-spatial-data/datasets-and-interfaces/product-descriptions/laser-scanning-data-5-p

Lehtonen I et al. 2019. Projected decrease in wintertime bearing capacity on different forest and soil types in Finland under a warming climate. Hydrol Earth Syst Sci. 23(3):1611–1631. https://doi.org/10.5194/hess-23-1611-2019

Metsäteho. 2017. [Forest road instructions. Classification of the bearing capacity of the subgrade.] Metsätieohjeisto. Pohjamaan kantavuusluokitus; [accessed 2024 Dec 16]. https://www.metsateho.fi/metsatieohjeisto/

Miller HJ, Kestler MA, Amatrudo M, Eaton R, Hall A. 2011. Comparison of test sections of low-volume roadways reconstructed with conventional techniques and full-depth reclamation. Transp Res Rec. 2204 (1):206–214. https://doi.org/10.3141/2204-26

Munro R. 2004. Dealing with bearing capacity problems on low volume roads constructed on peat. Including case histories from roads projects within the ROADEX partner districts. Roadex II. Northern Periphery; [accessed 2025 Jan 8]. https://www.roadex.org/wp-content/uploads/2014/01/2_5-Roads-on-Peat_l.pdf(openin a new window).

O'Mahony MJ, Ueberschaer A, Owende PMO, Ward SM. 2000. Bearing capacity of forest access roads built on peat soils. J Terramech. 37 (3):127–138. https://doi.org/10.1016/S0022-4898(00)00003-3

Open data 2026. Finnish Meteorological Institute; [accessed 2026 Jun 22]. https://en.ilmatieteenlaitos.fi/open-data-questions

papiNet. 2025. Data dictionary. Global standard for the paper and forest products supply chain. Build v2r31_20251015; [accessed 2025

Oct 23]. https://www.papinet.org/the-standard/download-current-version

Pinheiro J, Bates D. & R Core Team 2024. nlme: linear and nonlinear mixed effects models. R package version 3.1–166. https://CRAN.R-project.org/package=nlme

Pohjankukka J et al. 2025. Digital mapping of peat thickness and extent in Finland using remote sensing and machine learning. Geoderma. 455:117216. https://doi.org/10.1016/j.geoderma.2025.117216

R Core Team. 2024. R: a language and environment for statistical computing. R Foundation for Statistical Computing. https://www.R-project.org/

Saevarsdottir T, Erlingsson S. 2013. Water impact on the behaviour of flexible pavement structures in an accelerated test. Road Mater Pavement Des. 14(2):256–277. https://doi.org/10.1080/14680629.2013.779308

Stone M. 1974. Cross-validatory choice and assessment of statistical predictions. J R Stat Soc Ser B Stat Methodol. 36(2):111–133. https://doi.org/10.1111/j.2517-6161.1974.tb00994.x

Väätäinen K et al. 2025. Toward a digital twin of forest roads – road weather stations for monitoring road condition and trafficability in eastern Finland. Int J Eng. 37(2):211–224. https://doi.org/10.1080/14942119.2025.2533086

Waga K et al. 2020. Forest road status assessment using airborne laser scanning. For Sci. 66(4):501–508. https://doi.org/10.1093/forsci/fxz053

Waga K, Malinen J, Tokola T. 2021. Locally invariant analysis of forest road quality using two different pulse density airborne laser scanning datasets. Silva Fenn. 55(1):article id 10371. https://doi.org/10.14214/sf.10371

Yksityisteiden karttapalvelut [Data services for private roads] 2026. Finnish Forest Centre; [accessed 2026 Jun 22]. https://www.metsakeskus.fi/fi/metsan-kaytto-ja-omistus/yksityistiet/yksityisteiden-karttapalvelut